Journal of Neurology (2018) 265 (Suppl 1):S18–S25
https://doi.org/10.1007/s00415-018-8829-4

ORIGINAL COMMUNICATION

Pharmacological profile of vestibular inhibitory inputs to superior oblique motoneurons

Parthena Soupiadou[1,2] · Francisco Branoner[1] · Hans Straka[1]

Received: 2 February 2018 / Revised: 7 March 2018 / Accepted: 8 March 2018 / Published online: 19 March 2018

Abstract

Vestibulo-ocular reflexes (VOR) are mediated by three-neuronal brainstem pathways that transform semicircular canal and otolith sensory signals into motor commands for the contraction of spatially specific sets of eye muscles. The vestibular excitation and inhibition of extraocular motoneurons underlying this reflex is reciprocally organized and allows coordinated activation of particular eye muscles and concurrent relaxation of their antagonistic counterparts. Here, we demonstrate in isolated preparations of *Xenopus laevis* tadpoles that the discharge modulation of superior oblique motoneurons during cyclic head motion derives from an alternating excitation and inhibition. The latter component is mediated exclusively by GABA, at variance with the glycinergic inhibitory component in lateral rectus motoneurons. The different pharmacological profile of the inhibition correlates with rhombomere-specific origins of vestibulo-ocular projection neurons and the complementary segmental abundance of GABAergic and glycinergic vestibular neurons. The evolutionary conserved rhombomeric topography of vestibulo-ocular projections makes it likely that a similar pharmacological organization of inhibitory VOR neurons as reported here for anurans is also implemented in mammalian species including humans.

Keywords Vestibulo-ocular reflex · Semicircular canal · Extraocular motoneurons · GABA · Glycine

Introduction

Gaze stabilization during head/body motion depends to a large extent on vestibulo-ocular reflexes (VOR) [1]. The activation of spatio-temporally adequate eye movements derives from the transformation of semicircular canal and otolith sensory signals into extraocular motor commands within central vestibulo-ocular circuits [2]. The approximate topographical alignment between semicircular canal planes and eye muscle pulling directions [3] facilitates sensorimotor coordinate transformations within the brainstem circuitry [2]. The respective computations are performed along a principal three-neuronal pathway and include VIIIth nerve afferent fibers, central vestibular neurons and extraocular motoneurons [4]. The VOR circuitry is composed of reciprocal neuronal pathways that ensure simultaneous contractions of synergistic eye muscles and concurrent disfacilitation of their antagonists via crossed excitatory and uncrossed inhibitory vestibular projections onto extraocular motoneurons [2]. During vestibular-related gaze stabilization, the inhibition of respective extraocular motoneurons releases the contraction of antagonistic eye muscles and thereby ensures the exertion of compensatory eye movements with appropriate dynamics and amplitude.

This functional organization is evolutionarily conserved in all vertebrates with only few species-specific variations [5]. While the crossed excitatory vestibulo-ocular synaptic transmission is generally mediated by glutamate, the uncrossed vestibular inhibition appears to differ for horizontal and vertical/oblique extraocular motoneurons [2, 6]. Vestibular nerve-evoked disynaptic inhibitory inputs in abducens motoneurons are glycinergic as shown in cat [7]

Parthena Soupiadou and Francisco Branoner contributed equally to this study.

This manuscript is part of a supplement sponsored by the German Federal Ministry of Education and Research within the funding initiative for integrated research and treatment centers.

✉ Hans Straka
straka@lmu.de

[1] Department Biology II, Ludwig-Maximilians-University Munich, Großhaderner Str. 2, 82152 Planegg, Germany

[2] Graduate School of Systemic Neurosciences, Ludwig-Maximilians-University Munich, Großhaderner Str. 2, 82152 Planegg, Germany

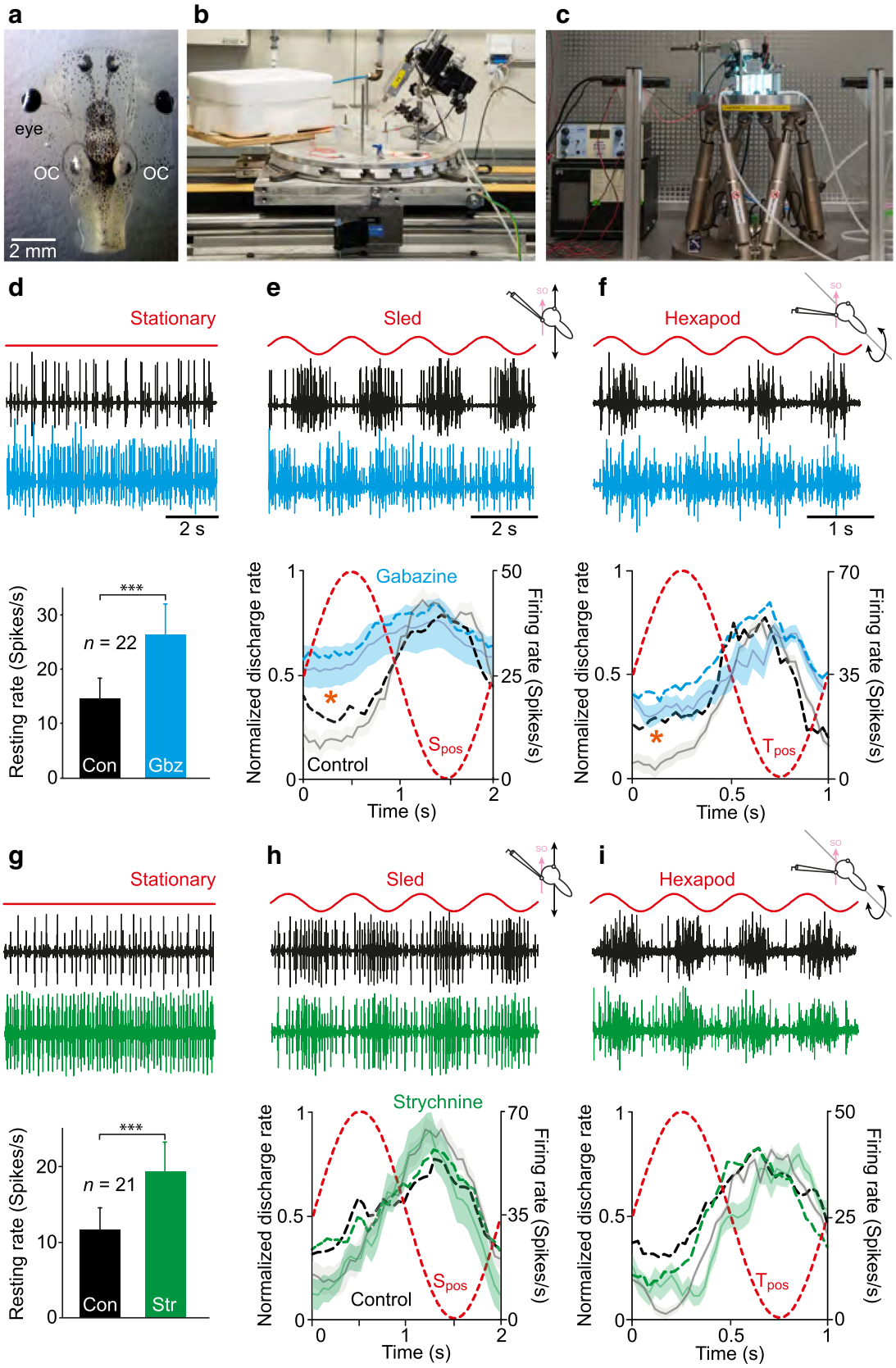
a
b
c
eye
OC
OC
2 mm
d
Stationary
2 s
e
Sled
2 s
f
Hexapod
1 s
Resting rate (Spikes/s)
***
n = 22
Con
Gbz
Gabazine
Control
Normalized discharge rate
Firing rate (Spikes/s)
Time (s)
Spos
Tpos
g
Stationary
h
Sled
i
Hexapod
n = 21
Con
Str
Strychnine
Control

◂**Fig. 1** Pharmacology of motion-evoked extraocular motor firing rate inhibition. **a–c** Image of an isolated preparation for SO nerve discharge recording (**a**) on a sled (**b**) and a Hexapod (**c**). **d–i** SO nerve multi-unit discharge in a stationary preparation (red line in **d**, **g**) and during sinusoidal horizontal translation (red sine wave in **e**, **h**) and roll motion (red sine wave in **f**, **i**) before (black traces) and during bath application of gabazine (2 μM; blue traces in **d–f**) and strychnine (10 μM; green traces in **g–i**); summary plots in **d, g** depict mean resting rates of isolated SO nerve single-units before and during bath application of gabazine (Gbz) and strychnine (Str); $***p<0.001$ (Wilcoxon signed-rank test) indicates the significance of difference; summary plots in **e**, **f**, **h**, **i** depict the average firing rate modulation over a single cycle (dashed red sine waves) of sled (**e**, **h**) and Hexapod motion (**f**, **i**) before (Control, gray and black curves) and during bath application of gabazine (blue curves) and strychnine (green curves); solid curves and light shaded areas represent the normalized mean firing rate ± SEM of the population of single-units before and during bath application of gabazine ($n=12$ in **e**; $n=10$ in **f**) and strychnine ($n=11$ in **h**; $n=10$ in **i**); firing rates in **e**, **f**, **h**, **i**, were normalized to the peak discharge before drug application; color-matched dashed curves represent the absolute firing rate of the typical examples shown in **e**, **f**, **h**, **i**, respectively; note the block of the inhibitory response component by gabazine (orange * in **e**, **f**); pictograms indicate the orientation of the preparation during translation and roll motion; the calibration bars in **d**, **e**, **f** also apply to **g**, **h**, **i**, respectively; *OC* otic capsule, S_{pos} sled position, T_{pos} table position

and frog [8] and the synaptic substrate for the cyclic disfacilitation of the lateral rectus nerve discharge during horizontal sinusoidal rotation [9]. In contrast, vestibular nerve-evoked disynaptic IPSPs in mammalian oculomotor motoneurons are GABAergic [10–12], compatible with the abundance of GABAergic terminals on the latter motoneurons in cat [13], goldfish [6] and primates [14]. The dynamics of glycine and $GABA_A$ receptor-mediated inhibitory responses is similar given that both receptors form chloride ion channels with comparable channel kinetics upon activation [15]. Therefore, it is unlikely that the employment of one or the other transmitter by the respective inhibitory VOR circuitry has a specific functional benefit. If the differential pharmacological organization of inhibitory vestibulo-ocular connections is indeed complementary with respect to glycine and GABA in the horizontal versus vertical/oblique extraocular motor system and also extends onto trochlear motoneurons is so far unknown. Accordingly, we determined the transmitter profile of the cyclic discharge disfacilitation of superior oblique motoneurons in *Xenopus laevis* tadpoles during oscillatory head motion in comparison with the known pharmacology of these responses in lateral rectus motoneurons [9].

Materials and methods

Animals and experimental preparation

Xenopus laevis tadpoles of either sex ($n=26$) at developmental stages 52–53 [16] were obtained from the in house animal breeding facility at the Biocenter-Martinsried of the Ludwig-Maximilians-University Munich. Tadpoles were maintained in tanks with non-chlorinated water (17–18 °C) at a 12/12 light/dark cycle. Experiments were performed in vitro on isolated preparations and comply with the "Principles of animal care", publication No. 86-23, revised 1985 of the National Institute of Health. Permission for these experiments was granted by the liable authority at the Regierung von Oberbayern (55.2-1-54-2532.3-59-12).

Tadpoles were anesthetized in 0.05% 3-aminobenzoic acid ethyl ester methanesulfonate (MS-222; Pharmaq Ltd. UK) in ice-cold frog Ringer solution (75 mM NaCl, 25 mM $NaHCO_3$, 2 mM $CaCl_2$, 2 mM KCl, 0.1 mM $MgCl_2$, and 11 mM glucose, pH 7.4) and decapitated at the level of the upper spinal cord. The skin above the head was removed, the cartilaginous skull was opened from dorsal, the forebrain disconnected and both optic nerves transected [9]. The remaining central nervous system and vestibular sensory periphery with its afferent connections and extraocular motoneuronal projections were functionally preserved (Fig. 1a). This allowed a natural activation of the linear and angular VOR on a sled (Tönnies, Switzerland; Fig. 1b) and a Hexapod (PI H-840, Physik Instrumente, Karlsruhe, Germany; Fig. 1c) under controlled in vitro conditions. Extraocular motor units were recorded from the trochlear nerve after its disconnection from the superior oblique (SO) target muscle by cutting the nerve close to the innervation site. For all experiments, preparations were placed in a Sylgard-lined recording chamber that was continuously superfused with oxygenated (Carbogen: 95% O_2, 5% CO_2) Ringer solution at a constant temperature of 17.0 ± 0.1 °C.

Electrophysiology and pharmacology

The recording chamber with the preparation affixed to the Sylgard floor was mounted onto a linear sled [17] or in the center of the rotation axes of a computer-controlled Hexapod (Fig. 1b, c). Spontaneous and motion-evoked spike discharge of the SO nerve was recorded extracellularly (EXT 10-2F; npi electronics; Tamm, Germany) with glass suction electrodes, digitized at 20 kHz (CED 1401, Cambridge Electronic Design, UK) and stored on computer for offline analysis. Suction electrodes were made from borosilicate glass (Science Products, Hofheim, Germany), pulled on a P-87 Brown/Flaming electrode puller. Electrode tips were individually broken to fit the size of the SO nerve. Individual motor units were isolated from the multi-unit recordings using spike amplitude. A modulation of SO nerve activity was elicited by sinusoidal rotations and linear translations along a direction formed by the functional ipsilateral posterior (PC) and contralateral anterior vertical semicircular canal (AC) pair [17]. Stimuli were applied at 1 Hz and

peak velocity amplitude of ± 10°/s for angular and 0.5 Hz and ± 5 cm for linear motion.

An implication of glycine and GABA in head/body motion-evoked inhibition of SO motoneuronal activity was tested by bath application of the glycine receptor blocker strychnine hydrochloride (10 µM; Tocris Bioscience, UK) and the $GABA_A$ receptor blocker gabazine (2 µM; Tocris Bioscience, UK), dissolved in frog Ringer solution. These experiments were supplemented by focal pressure pulse injections (0.5 bar; 50–80 ms) of ~ 50 nl strychnine (10 µM) and gabazine (20 µM) into the trochlear nucleus through beveled (30°) glass microelectrodes with a tip diameter of ~ 20 µm [9]. Based on landmarks, such as the midline and the cerebellum, electrodes were inserted with a micromanipulator from dorso-caudal through the ventricular surface into the trochlear nucleus [18].

Data analysis

Peri-stimulus time histograms (PSTHs) of average SO nerve firing patterns over a single head motion cycle were obtained from raw data using Spike2 scripts that allowed extracting the firing patterns of single units. Average responses were calculated from at least 10 cycles. The PSTHs were further processed and analyzed statistically using Microcal Origin 6.0G (OriginLab Corp., USA). PSTHs were normalized and averaged (± SEM; standard error of the mean) for comparison. Statistical differences were calculated with the Wilcoxon signed-rank test (paired parameters; Prism, Graphpad Software, Inc, USA).

Results

Spontaneous and motion-evoked discharge of SO motor units

The discharge of SO motoneurons at rest, during horizontal linear translation and roll motion was obtained in vitro by recording the spike activity of the trochlear nerve after disconnection from its SO target muscle (Fig. 1a). The spike activity of isolated, single SO nerve fibers (black traces in Fig. 1d, g) was variable between different units with an average resting rate of ~ 15 spikes/s (14.8 ± 2.7 spikes/s; mean ± SEM; $n = 61$). Sinusoidal translational motion (0.5 Hz; ± 5 cm) on a sled caused a robust cyclic discharge modulation that was phase-coupled to the stimulus (black traces in Fig. 1e, h). The modulation depth was maximal during linear translation along a plane formed by the ipsilateral PC—contralateral AC (see pictograms in Fig. 1e, h) [15] and reached an average peak firing rate of ~ 45 spikes/s (46.3 ± 4.8 spikes/s; mean ± SEM; $n = 29$). Sinusoidal roll motion (1 Hz; ± 10°/s) on a Hexapod along the same semicircular canal plane (see pictograms in Fig. 1f, i) also caused a robust discharge modulation (black traces in Fig. 1f, i) with an average peak rate of ~ 50 spikes/s (51.3 ± 5.3 spikes/s; mean ± SEM; $n = 32$). The robust modulation of SO nerve motor units during translation and roll motion is illustrated in the plot of Fig. 1e, f and serves in the subsequent pharmacological experiments as control to evaluate the impact of GABA and glycine in the cyclic modulation of vestibular inputs in SO motoneurons.

Bath application of gabazine and strychnine

The cyclic discharge of SO nerve fibers during sinusoidal translation or roll motion complies with a reciprocal vestibular excitation and inhibition of extraocular motoneurons [2]. The inhibition could be either glycineric as in abducens motoneurons [9] or GABAergic as shown for cat [12] or goldfish oculomotor motoneurons [6]. We tested the pharmacological profile of the cyclic disfacilitation of SO motoneuronal firing during sinusoidal head motion by application of the selective $GABA_A$-receptor blocker gabazine and the glycine-receptor blocker strychnine. Following bath application of 2 µM gabazine, the resting rate of SO nerve fibers in stationary preparations (14.6 ± 3.8 spikes/s; mean ± SEM; $n = 22$ from 9 preparations) started to increase ~ 8 min after arrival of the drug in the bath and saturated at an elevated level after ~ 15 min (compare black and blue traces in Fig. 1d). The average resting rate in the presence of gabazine increased by 80% to 26.4 ± 5.7 spikes/s and was significantly different ($p < 0.0001$; Wilcoxon signed-rank test) from the control resting rate (plot in Fig. 1d). During sinusoidal translation ($n = 12$) or roll motion ($n = 10$), the discharge modulation of SO nerve fibers (black traces in Fig. 1e, f) became less prominent in the presence of gabazine (blue traces in Fig. 1e, f). As confirmed by calculating the average response over a single motion cycle (plots of Fig. 1e, f), the reduction is due to a diminishment of the inhibitory component. This latter effect becomes clearly visible by comparing pre- and post-application responses of the representative example (black/blue dashed curves in the plots of Fig. 1e, f) as well as in the population average (light shaded areas and orange * in the plots of Fig. 1e, f). The statistical comparison yielded a significant difference ($p < 0.01$; Wilcoxon signed-rank test) in the magnitudes of the inhibitory component independent of the motion paradigm (compare plots in Fig. 1e, f), suggesting that semicircular canal and otolith pathways employ GABA as transmitter.

Bath application of 10 µM strychnine also increased the resting rate of SO nerve fibers in stationary preparations from 11.6 ± 2.9 to 19.2 ± 4.0 spikes/s (mean ± SEM; $n = 21$ from 9 preparations; plot in Fig. 1g). This increase by more than 65% was significant ($p < 0.001$; Wilcoxon signed-rank test) compared to the control firing rate before drug

application and qualitatively comparable to the effect of gabazine (compare plots in Fig. 1d, g). However, in contrast to gabazine, bath application of strychnine failed to alter the dynamics of the SO nerve discharge modulation during sinusoidal translation ($n = 11$) or roll motion ($n = 10$) as illustrated by the two typical motor units in Fig. 1h and i (compare black and green traces, respectively). This impression was confirmed at the population level by calculating the average response over a single motion cycle before and during strychnine application (plots in Fig. 1h, i). The absence of a strychnine-mediated impairment of the cyclic disfacilitation suggests that glycine is not involved in the vestibulo-ocular inhibition of SO motoneurons.

Focal injections of gabazine and strychnine into the trochlear nucleus

Bath application of transmitter antagonists is convenient to reliably block synaptic transmission with a defined concentration of a specific drug, however, it does not allow to target a particular synaptic connection. Therefore, we pressure-injected small volumes of gabazine or strychnine [9] into the trochlear nucleus to directly block inhibitory inputs to SO motoneurons (Fig. 2a). Injection of ~ 50 nl gabazine (20 µM) caused a reversible increase of the resting discharge of SO nerve fibers (Fig. 2b). As illustrated in the typical example in Fig. 2b, the augmentation of the firing rate from ~ 10 spikes/s (10.1 ± 2.0; mean ± SEM; $n = 13$ from 4 preparations) in controls occurred within 2–5 s, to reach an elevated level of ~ 17 spikes/s (16.7 ± 3.5 spikes/s). This rate was maintained for about 10–30 s and slowly decayed over a period of 20–30 s (orange trace in Fig. 2b). The transient increase in firing rate was variable but significant at the population level ($p < 0.001$; Wilcoxon signed-rank test). The average magnitude by which injected gabazine elevated the spontaneous discharge (~ 60%) was smaller than after bath application, likely due to the localized block of inhibitory inputs at the level of SO motoneurons. Focal injection of gabazine into the trochlear nucleus during roll motion reduced the amplitude of the cyclic SO nerve fiber discharge (orange trace in Fig. 2c) in a comparable fashion as after bath application of this drug. Comparison of the modulation before (Fig. 2d) and after gabazine injection (Fig. 2e) indicated that the smaller discharge oscillation is due to a loss of discharge disfacilitation. Calculation of the average response over a single motion cycle (compare solid black and blue curves in Fig. 2f) illustrated in fact a lack of discharge disfacilitation in the presence of gabazine (orange * in Fig. 2f). This was confirmed by the statistical comparison that yielded a significant difference in the magnitude of the inhibitory component ($p < 0.001$; Wilcoxon signed-rank test).

In a complementary set of experiments, focal injections of ~ 50 nl strychnine (10 µM) into the trochlear nucleus transiently augmented the resting discharge of SO nerve fibers from 11.1 ± 1.7 spikes/s (mean ± SEM) to 16.7 ± 2.1 spikes/s ($n = 6$ from 4 preparations) with a similar dynamics as gabazine (see above). The extent (~ 50%) and temporal progression of the strychnine-induced increase and subsequent decrease of the spontaneous discharge was also similar to that after focal injections of gabazine. In contrast, strychnine had no effect on the magnitude of the cyclic discharge of SO nerve motor units during translational motion ($n = 6$; not shown), as already observed during bath application of this drug (see Fig. 1h, i). In fact, the inhibitory component of SO nerve discharge modulation remained entirely unchanged in the presence of strychnine in the trochlear nucleus.

Discussion

Vestibular-evoked cyclic disfacilitation of the SO neve discharge during sinusoidal angular rotation and linear translation was completely blocked by bath application or local injection of the $GABA_A$-receptor antagonist gabazine into the trochlear nucleus, whereas the glycine-receptor blocker strychnine had no effect. Thus, vestibular inhibitory inputs in SO motoneurons have a different pharmacological profile as those in lateral rectus motoneurons.

The complete block of the inhibitory component of the SO nerve discharge during sinusoidal motion by gabazine indicates that this response component derives from a vestibular inhibition rather than from a mere disfacilitation of the excitatory response. This 'push–pull' organization, therefore, complies with the general functional principle of VOR pathways that consists of a reciprocal synaptic excitation and inhibition from spatially opposing semicircular canal and utricular epithelial areas [2, 5]. However, at variance with the semicircular canal-evoked glycinergic vestibular inhibition of abducens motoneurons in *Xenopus laevis* [9], trochlear motoneurons in this species receive a vestibular inhibition exclusively via GABA (Fig. 2b–e). The different transmitter profile in *Xenopus* is thus similar to that of mammalian oculomotor and abducens motoneurons [7, 10–12]. Therefore, the differential employment of GABA and glycine in the inhibition of extraocular motoneurons appears to be an evoluntionary conserved vertebrate feature. While this pharmacological differentiation of inhibitory VOR profiles with respect to the spatial plane of sensory signals and/or eye movements represents an appealing organizational principle, its evolutionary origin is likely not related to a vectorial reference frame per se. Rather, it emerges from the initial evolutionary blueprint of vestibular networks in early vertebrates [5].

The differential pharmacological profile of the vestibular inhibition in abducens (glycine) versus oculomotor/

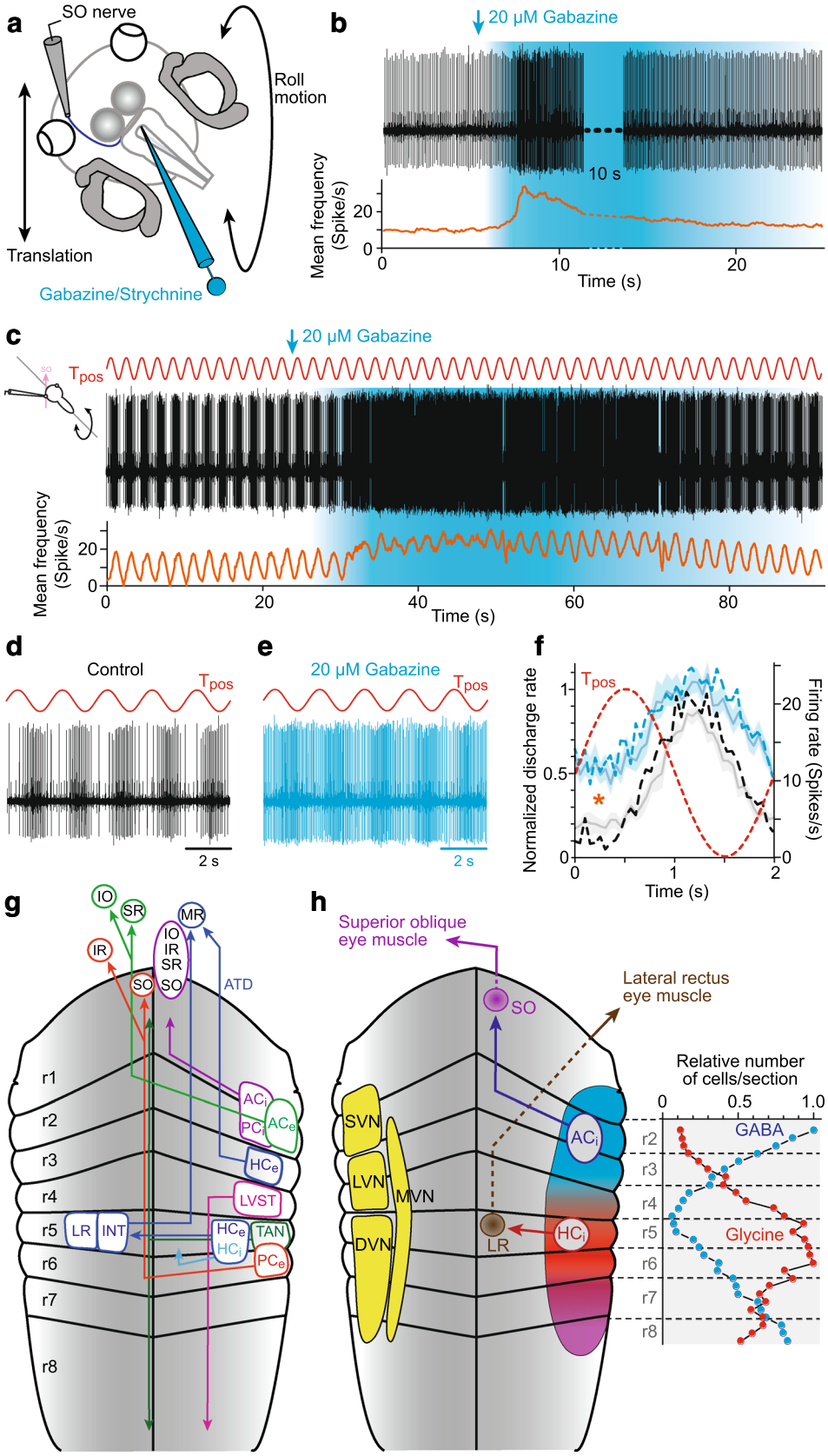
a
SO nerve
Roll motion
Translation
Gabazine/Strychnine
b
20 µM Gabazine
10 s
Mean frequency (Spike/s)
Time (s)
c
20 µM Gabazine
Tpos
Mean frequency (Spike/s)
Time (s)
d
Control
Tpos
2 s
e
20 µM Gabazine
Tpos
2 s
f
Tpos
Normalized discharge rate
Firing rate (Spikes/s)
Time (s)
g
IO
SR
MR
IR
IO IR SR SO
SO
ATD
r1
r2
r3
r4
r5
r6
r7
r8
ACi
PCi
ACe
HCe
LVST
LR
INT
HCe
HCi
TAN
PCe
h
Superior oblique eye muscle
Lateral rectus eye muscle
SO
SVN
LVN
MVN
DVN
LR
ACi
HCi
Relative number of cells/section
GABA
Glycine
r2
r3
r4
r5
r6
r7
r8

◂**Fig. 2** Pharmacological profile of inhibitory horizontal and vertical/oblique VOR connections. **a** Schematic of a semi-intact *Xenopus* preparation depicting the SO nerve recording, pressure injection of transmitter blocker into the trochlear nucleus (blue pipette) and directions of translational and roll motion. **b–e** Isolated SO nerve discharge in a stationary preparation (**b**) and during sinusoidal roll motion (**c**) before (**d**) and after focal injection of gabazine (20 µM) into the trochlear nucleus (**e**); the pictogram in **c** indicates the orientation of the preparation during sinusoidal roll motion (red curves in **c–e**); blue-colored areas in **b**, **c** indicate the tentative drug dynamics; orange curves in **b**, **c** indicate the mean frequency (bin width: 100 ms) of the discharge. **f** normalized average firing rate modulation of all SO nerve motor units ($n = 13$) over a single cycle (dashed red sine wave) before (black curve) and during gabazine injection (blue curve); solid curves and gray/light blue shaded areas represent the normalized (relative to the peak discharge before drug injection) mean firing rate ± SEM of the population of single-units before and during drug application; color-matched dashed curves represent the absolute firing rate of the typical example shown in **b-e**; note the block of the inhibitory response component by gabazine (orange *). **g**, **h** Schematics of the rhombomeric scaffold summarizing locations and bilateral projections of vestibulo-ocular and vestibulospinal projection neurons (**g**), the separation into classical vestibular nuclei (yellow in **h**) and the rostro-caudal distribution of GABAergic (blue in **h**) and glycinergic vestibular neurons (red in **h**); vestibulo-ocular projections and extraocular motoneuronal targets in **g** are color-coded; the rostro-caudal distribution of GABAergic and glycinergic vestibular neurons (right plot in **h**) was adapted from [21]. $AC_{e,i}$, $PC_{e,i}$ anterior, posterior vertical semicircular canal excitatory and inhibitory neurons, *ATD* ascending tract of Deiters, *DVN, LVN, MVN, SVN* descending, lateral, medial, superior vestibular nucleus, $HC_{e,i}$ horizontal semicircular canal excitatory and inhibitory neurons, *INT* abducens internuclear neurons, *IO, SO* inferior, superior oblique motoneurons, *IR, SR* inferior, superior rectus motoneurons, *LR, MR* lateral, medial rectus motoneurons, *LVST* lateral vestibulo-spinal tract, *r1–8* rhombomere 1–8, *TAN* tangential vestibular neurons, T_{pos} table position

trochlear motoneurons (GABA) is likely due to the origin of the respective population of vestibulo-ocular projection neurons in the hindbrain [2, 5]. In all vertebrates, the hindbrain is longitudinally structured as a series of individual segments, the rhombomeres (r) [2]. While rhombomeres are visible at the gross morphological level only in embryos, the intrinsic overall topography of the segmental patterning is retained throughout life as reflected by the rostro-caudal location of, e.g. cranial motoneurons or vestibular projection neurons [5]. The identity of a given hindbrain segment and its subcompartments derives from unique combinatorial expression patterns of genes for transcriptional factors and cell signaling molecules, thereby defining the phenotype of the cells located within each rhombomere [18]. According to this genetic definition of functional phenotypes along the rostro-caudal extent of the hindbrain segmental scaffold, the topographic premotor/motor organization of vestibular projection neurons generates a framework within which vestibulo-ocular neurons originate from specific segmental postions [5]. Most notably, the emerging rhombomeric arrangement of distinct, target-specific populations of vestibular projection neurons represents a hodological mosaic that is highly conserved throughout vertebrates [5, 19]. Each population of semicircular canal-related excitatory and inhibitory vestibulo-ocular projection neurons derives from a particular hindbrain segment (Fig. 2g) [5, 18]. Accordingly, inhibitory oculomotor and trochlear nucleus-projecting vestibulo-ocular neurons derive from r2–3 (Fig. 2g). In contrast, inhibitory abducens nucleus-projecting vestibulo-ocular neurons originate from r5 to form a homo-segmental connection with abducens motoneurons and internuclear neurons that in anurans also derive from r5 [18, 20].

GABAergic and glycinergic vestibular neurons also exhibit a differential, hindbrain segment-specific regional distribution as demonstrated in adult frogs (right plot in Fig. 2h) [21]. GABAergic vestibular neurons are abundant in r1–r4 and r7–8, but rather scarce in r5–6 (blue area in Fig. 2h). In contrast, glycinergic vestibular neurons occur predominantly in r5–6, whereas the adjacent rostral and caudal segments are devoid or contain considerably fewer neurons of this phenotype. Thus, GABAergic and glycinergic vestibular neurons are organized in a complementary, segment-specific fashion along the rostro-caudal extent of the hindbrain. The consequently differential availability of the two inhibitory transmitter phenotypes along the rhombomeric scaffold [20] together with the distinct segmental origin of inhibitory vestibulo-ocular projection neurons from r2–3 and r5, respectively [18] is, therefore, the likely decisive factor for the differential employment of GABA and glycine as inhibitory transmitters in the vertical/oblique versus the horizontal VOR, respectively. While this functional organization has been demonstrated in anurans [2], circumstantial anatomical, immuno-histochemical and developmental evidence suggests that the same rhombomere-specific principle also applies to mammalian species, including humans [22–24]. Accordingly, any pharmacological difference in the organization of 3d-VOR pathways is likely related to the topographic framework within which the individual elements of the circuitry are formed during development.

The differential employment of GABA and glycine in the vertical/oblique and horizontal VOR represents an interesting, clinically relevant condition given that GABAergic drugs are frequently used for the treatment of symptoms such as anxiety disorder, epilepsy or spasticity [25]. Accordingly, it is tempting to speculate that the pharmacolocial application of benzodiazepines, barbiturates or certain anesthetics might also cause eye movement disturbances or pathological motion illusions in the vertical but not in the horizontal plane. An interesting, testable hypothesis, therefore, is that GABAergic drugs differentially impair vertical and horizontal eye movements, a prediction that can be well studied in the respective populations of human subjects. More specifically, a pharmacological manipulation of $GABA_A$ receptors should predominantly affect vertical eye movements evoked by slow tonic extraocular motoneurons,

assuming a comparable differential organization as shown for the glycinergic vestibular inhibition of tonic but not phasic abducens motoneurons [9]. A clear answer, however, might be masked by the fact that GABA is also the predominant transmitter of the vestibular commissural and exclusive transmitter of the cerebellar Purkinje cell-mediated inhibition of vestibulo-ocular neurons, independent of the target extraocular motoneurons. Nonetheless, patients that receive GABAergic drugs, either acutely or chronically, form an excellent clinical test population to study a potentially selective pharmacological modification of direction-specific eye movements in humans.

Acknowledgements The authors acknowledge financial support from the German Science Foundation (CRC 870; STR 478/3-1) and the German Federal Ministry of Education and Research under the Grant code 01 EO 0901. The authors thank Kathrin Gensberger for the technical support in part of the experiments and Dr. Boris Chagnaud for constructive comments on the manuscript.

Compliance with ethical standards

Conflicts of interest The authors declare no competing financial interests.

Ethical standard The study was performed in accordance with the ethical standards statement.

References

1. Angelaki DE, Cullen KE (2008) Vestibular system: the many facets of a multimodal sense. Annu Rev Neurosci 31:125–150
2. Straka H, Fritzsch B, Glover JC (2014) Connecting ears to eye muscles: evolution of a 'simple' reflex arc. Brain Behav Evol 83:162–175
3. Graf W, Simpson JI (1981) The relations between the semicircular canals, the optic axis, and the extraocular muscles in lateral-eyed and frontal-eyed animals. In: Fuchs A, Becker W (eds) Progress in oculomotor research, developments in neuroscience, vol 12. Elsevier, New York, pp 411–420
4. Branoner F, Chagnaud BP, Straka H (2016) Ontogenetic development of vestibulo-ocular reflexes in amphibians. Front Neural Circuits 10:91
5. Straka H, Baker R (2013) Vestibular blueprint in early vertebrates. Front Neural Circuits 7:182
6. Graf W, Spencer R, Baker H, Baker R (1997) Excitatory and inhibitory vestibular pathways to the extraocular motor nuclei in goldfish. J Neurophysiol 77:2765–2779
7. Spencer RF, Wenthold RJ, Baker R (1989) Evidence for glycine as an inhibitory neurotransmitter of vestibular, reticular, and prepositus hypoglossi neurons that project to the cat abducens nucleus. J Neurosci 9:2718–2736
8. Straka H, Dieringer N (1993) Electrophysiological and pharmacological characterization of vestibular inputs to identified frog abducens motoneurons and internuclear neurons in vitro. Eur J Neurosci 5:251–260
9. Dietrich H, Glasauer S, Straka H (2017) Functional organization of vestibulo-ocular responses in abducens motoneurons. J Neurosci 37:4032–4045
10. Ito M, Highstein SM, Tsuchiya T (1970) The postsynaptic inhibition of rabbit oculomotor neurons by secondary vestibular impulses and its blockage by picrotoxin. Brain Res 17:520–523
11. Obata K, Highstein SM (1970) Blocking by picrotoxin of both vestibular inhibition and GABA action on rabbit oculomotor neurons. Brain Res 18:538–541
12. Precht W, Baker R, Okada Y (1973) Evidence for GABA as the synaptic transmitter of the inhibitory vestibulo-ocular pathway. Exp Brain Res 18:415–428
13. De la Cruz RR, Pastor AM, Martinez- Guijarro FJ, Lopez-Garcia C, Delgado-Garcia JM (1992) Role of GABA in the extraocular motor nuclei of the cat: a postembedding immunocytochemical study. Neuroscience 51:911–929
14. Zeeh C, Mustari MJ, Hess BJM, Horn AKE (2015) Transmitter inputs to different motoneuron subgroups in the oculomotor and trochlear nucleus in monkey. Front Neuroanat 9:95
15. Jentsch TJ (1996) Chloride channels: a molecular perspective. Curr Opin Neurobiol 6:303–310
16. Nieuwkoop PD, Faber J (1994) Normal Table of *Xenopus Laevis* (Daudin): a systematical and chronological survey of the development from the fertilized egg till the end of metamorphosis. Garland Pub, New York
17. Branoner F, Straka H (2015) Semicircular canal-dependent developmental tuning of translational vestibulo-ocular reflexes in *Xenopus laevis*. Dev Neurobiol 75:1051–1067
18. Straka H, Baker R, Gilland E (2001) Rhombomeric organization of vestibular pathways in larval frogs. J Comp Neurol 437:42–55
19. Díaz C, Glover JC (2002) Comparative aspects of the hodological organization of the vestibular nuclear complex and related neuron populations. Brain Res Bull 57:307–312
20. Straka H, Holler S, Goto F, Kolb FP, Gilland E (2003) Differential spatial organization of otolith signals in frog vestibular nuclei. J Neurophysiol 90:3501–3512
21. Reichenberger I, Straka H, Ottersen OP, Streit P, Gerrits NM, Dieringer N (1997) Distribution of GABA, glycine and glutamate immunoreactivities in the vestibular nuclear complex of the frog. J Comp Neurol 377:149–164
22. Walberg F, Ottersen OP, Rinvik E (1990) GABA, glycine, aspartate, glutamate and taurine in the vestibular nuclei: an immunocytochemical investigation in the cat. Exp Brain Res 79:547–563
23. Büttner-Ennever JA (1992) Patterns of connectivity in the vestibular nuclei. Ann NY Acad Sci 656:363–378
24. Pasqualetti M, Díaz C, Renaud J-S, Rijli FM, Glover JC (2007) Fate-mapping the mammalian hindbrain: segmental origins of vestibular projection neurons assessed using rhombomere-specific Hoxa2 enhancer elements in the mouse embryo. J Neurosci 27:9670–9681
25. Jembrek MJ, Vlainic J (2015) GABA receptors: pharmacological potential and pitfalls. Curr Pharm Des 21:4943–4959